INFLOW CONDITIONS FOR LARGE-EDDY SIMULATION USING A NEW VORTEX METHOD

Nicolas Jarrin
School of Mechanical, Aerospace and Civil Engineering,
The University of Manchester, Manchester, UK
N.Jarrin@postgrad.umist.ac.uk

Sofiane Benhamadouche
Département Mécanique des Fluides et Transferts Thermiques,
Electrictié de France,6 quai Watier, Chatou, France
sofiane.benhamadouche@edf.fr

Dominique Laurence
School of Mechanical, Aerospace and Civil Engineering,
The University of Manchester, Manchester, UK
dominique.laurence@manchester.ac.uk

ABSTRACT

The generation of inflow data for spatially evolving turbulent flows is one of the challenging problems for the use of LES on industrial flows and complex geometries. A new method of generation of synthetic turbulence suitable for complex geometries and unstructured meshes is presented herein. The method is based on the classical view of turbulence as a superposition of coherent structures. It is able to reproduce prescribed first and second order one point statistics, characteristic length and time scales as well as the shape of coherent structures. The ability of the method to produce realistic inflow conditions on the test cases of the spatially decaying homogeneous isotropic turbulence, the non-periodic turbulent channel flow and the planar asymmetric diffuser is surveyed. The method is systematically compared to other methods of generation of inflow condition (precursor simulation, spectral method, basic random procedure)

INTRODUCTION

It is widely accepted that the specification of realistic inlet boundary conditions play a major role in the accuracy of a numerical simulation. For RANS approaches, only mean profiles for the velocity and the turbulent variables need to be prescribed which makes the definition of inflow data rather straight-forward. For large-eddy and direct-numerical simulations, this generation of inflow data is much more of an issue as turbulent unsteady inflow conditions have to be prescribed. It was shown that the results of DNS or LES of a plane jet (Klein et al., 2003), a spatially developing boundary layer (Lund et al., 1998) or a backward facing step (Jarrin et al., 2003) are very sensitive to inflow conditions.

A very effective way to avoid this problem is the use of periodic boundary conditions but this technique is restricted to a few simple geometries and test cases. From an engineering point of view, almost all industrial flows require the use of inlet boundary conditions. The need for methods to generate realistic unsteady inflow conditions is then mandatory to use LES in industrial cases with a certain degree of confidence in the results.

The most accurate technique consists in obtaining inflow data from a precursor simulation. However this technique has two major drawbacks. Firstly, it is restricted to simple cases where the flow at the inlet of the computational domain can be regarded as a fully developed turbulent flow (Kaltenbach et al., 1999) or a turbulent boundary layer (Lund et al., 1998). If the flow at the inlet is not explicitly specified and tests on turbulence intensity, length-scales of the inflow are to be made, this method is not suitable. Secondly, it entails a heavy extra computational load. Moreover in the scope of performing embedded LES, this approach is not suitable either. Thus the research effort seems to head towards methods of generation of synthetic turbulence.

The basic and still widely used technique to generate turbulent inflow data is to take a mean velocity profile with superimposed random fluctuations. The data generated do not exhibit any spatial or temporal correlations. The energy generated is uniformly spread in all wave numbers and therefore due to a lack of energy in the low wave number range, the pseudo turbulence is quickly dissipated (Jarrin et al., 2003).

A standard method to give some spatial and temporal correlations to the generated data is to create time series of velocity fluctuations by performing an inverse Fourier transform for prescribed spectral densities (Lee et al., 1992 or Kondo et al., 1997). Even though these methods were applied with success for the simulation of isotropic homogeneous turbulence or a backward facing-step they have several drawbacks which make them not suitable for industrial purposes. Indeed they are derived for periodic signals on uniform meshes. On

complex inlet meshes where fast fourier transform cannot be used, they become really expensive and not really appropriate. Moreover it uses 3D energy spectrum or power spectral density that we often cannot provide and it is not clear if different spectra can be used at different position in the flow to simulate non-homogeneous turbulence.

A more efficient technique for arbitrary inlet meshes is to filter random data on the inlet mesh (Klein et al., 2003). Gaussian filters have been used to generate inflow data with spatial and temporal correlations. To get more insight into the flow physics, Druault et al. (2004) used a proper-orthogonal-decomposition of a turbulent signal coming from experimental or numerical data and use this compressed signal as an inflow condition for LES calculation. Even though this technique cannot be applied systematically for any flow as it requires a previous realization of the flow, it is interesting to note that a better simulation of the coherent structures of the flow at the inlet enables a better simulation of the downstream flow.

The method presented in this paper is based on the classical view of turbulence as a superposition of eddies. The idea behind the method is to directly focus on prescribing coherent structures rather than reverting straight to spectral methods. It is an extension to the previous work of Jarrin et al. (2003) which used streamwise vortices to trigger turbulence downstream the inlet of a LES calculation. The final method presented herein is very easy to implement, very fast to run, performs well on any geometry and any kind of flow. The data generated exhibit very good physical properties such as first and second order one point statistics as well as prescribed length scales, time scales and shape of autocorrelation functions.

INFLOW GENERATION METHOD

The method is based on the classic view of turbulence as a superposition of coherent structures or turbulent spots. Coherent structures will be generated over the inlet plane of our calculation and it will be defined by a shape function defining its spatial and temporal characteristics.

We start by the one-dimensional case where a one component velocity signal has to be generated on the interval $[a,b]$. $f(x)$ is the shape function of the turbulent spot with a compact support $[-\sigma,\sigma]$ satisfying the normalization condition

$$\frac{1}{\Delta}\int_{-\Delta/2}^{\Delta/2} f_\sigma^2(x)dx = 1 \tag{1}$$

where $\Delta = b-a+2\sigma$. Each turbulent spot i has a position x_i (defining its physical position) and a length scale σ_i (defining its spectral content). For sake of simplicity, we will keep a constant σ for the moment. The issue of non-constant length-scale σ will be tackled later. Each spot is assigned a sign ε_i. Thus the contribution $u^{(i)}(x)$ of turbulent spot i to the velocity field is

$$u^{(i)}(x) = \varepsilon_i f_\sigma(x-x_i) \tag{2}$$

where ε_i is a random step of value $+1$ or -1 and x_i is drawn randomly on the interval $[a-\sigma, b+\sigma]$. The velocity signal at a point x is the sum of the contribution of all turbulent spots on the domain. For N turbulent spots it reads

$$u(x) = \frac{1}{\sqrt{N}}\sum_{i=1}^{N} \varepsilon_i f_\sigma(x-x_i) \tag{3}$$

The number of vortices on the domain can be set to $(b-a)/\sigma$ which ensures that the plane remains statistically covered with turbulent spots.

It can readily be shown then that our signal is of zero mean, unite variance and that the two-points autocorrelation function reads

$$R_{uu}(r) = \frac{1}{b-a}\int_a^b f_\sigma(x) f_\sigma(x+r)dx \tag{4}$$

The generalisation of the 1D procedure to the 3D case is very straight-forward. The shape function f_j associated to the j^{th} component of the velocity signal is now a function of the three coordinates (y,z,t) with a compact support $[-\sigma_y,\sigma_y;-\sigma_z,\sigma_z;-\sigma_t,\sigma_t]$ satisfying a 3D normalization condition. The signal at a point (y,z) and a time t in the inlet flow plane reads

$$u_j(\underline{x},t) = \frac{1}{\sqrt{N}}\sum_{i=1}^{N} u^{(i)(j)}(\underline{x},t) \tag{5}$$

with the contribution of vortex i to component j being

$$u^{(i)(j)}(\underline{x},t) = \varepsilon_{ij} f_j(y-y_i, z-z_i, t-t_i) \tag{6}$$

where ε_{ij} is the sign of vortex i on component j and are again independent random steps. To avoid the domain being empty of turbulent spots, the number of active turbulent spots N (a spot for which $|t-t_i| < \sigma_t$) on the inlet plane is kept constant and can be approximated by S_p/S_s where S_p is the surface of the inlet plane and S_s the surface of the support of a turbulent spot. Thus the plane remains statistically covered with turbulent spots.

The independence of the rotation sign ensures that our inflow signal satisfies the condition $\overline{u_i u_j} = \delta_{ij}$. The choice of the shape function determines the nature of the two-points autocorrelation function $R_{ii}(r_1,r_2,\tau)$. It reads

$$\frac{1}{S_p}\frac{1}{T}\int_{S_p}\int_0^T f_i(y,z,t) f_i(y+r_1, z+r_2, t+\tau)dydzdt \tag{7}$$

If the Reynolds stress tensor R_{ij} and the mean velocity profile $\overline{u_i}$ are known *a priori* from previous experiments, DNS or RANS calculations, our signal can be transformed to match these statistics (Lund et al., 1998). The final velocity field $u_i^{(f)}$ is then reconstructed from the vortex field $u_i^{(v)}$ according to

$$u_i^{(f)} = \overline{u_i} + a_{ij} u_j^{(v)} \tag{8}$$

where a_{ij} is obtained from the prescribed Reynolds stress tensor and reads

$$\begin{pmatrix} \sqrt{R_{11}} & 0 & 0 \\ R_{21}/a_{11} & \sqrt{R_{22}-a_{21}^2} & 0 \\ R_{31}/a_{11} & (R_{32}-a_{21}a_{31})/a_{22} & \sqrt{R_{33}-a_{31}^2-a_{32}^2} \end{pmatrix} \tag{9}$$

The length scale in the flow can also be varied even though the formulae (7) is only correct for a constant σ. Space varying σ introduces deformations to the autocorrelations function which become more important as the variations of σ get steeper. This is clearly one advantage of our method compared to spectral methods. The compact support of the spots enables us to make the spectral content of the shape function

vary in space which might be of great interest to simulate wall flows. The structures of the flow can also be controlled in order to have streamwise counter rotating-vortices at the wall fo a channel flow. In the following the method will thus be referred to as the Synthetic eddy method (SEM).

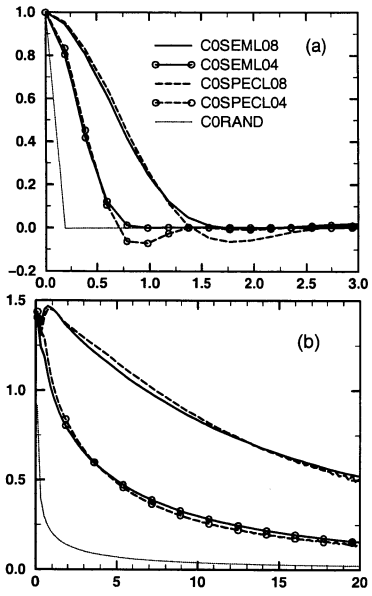

Figure 1: Spatially decaying isotropic turbulence (a) Longitudinal autocorrelation function of the inflow data (b) Evolution of the turbulent kinetic energy downstream the inlet

Code_Saturne, a collocated finite volume code for complex geometries (Archambeau et al., 2003) is used. Velocity and pressure coupling is ensured by a prediction/correction method with a SIMPLEC algorithm. The collocated discretisation requires a Rhie and Chow (1982) interpolation in the correction step to avoid oscillatory solutions. A second order centered scheme (in space and time) is used.

SPATIALLY DECAYING ISOTROPIC TURBULENCE

The first test carried out corresponds to the most basic test we can impose to our method. The turbulence is only determined by the boundary conditions so the evolution of the structures generated can be tracked readily.

The mean flow is in the positive x direction. The mesh dimensions are $2\pi \times 2\pi \times 8\pi$. The mesh is homogeneous is all three direction and has $32 \times 32 \times 128$ cells. Periodic boundary conditions are used in the y and z direction. The Smagorinsky constant is set to its theoretical value $C_S = 0.18$. The independent parameters defining the calculation are the viscosity ν, the turbulent energy k and the integral length scale L. The first two parameters are $\nu = 3.510^{-4}$ and $k = 1.5$ which leaves only one free parameter, the length scale to define the Reynolds number. The simulations carried out using different length scales and different methods are listed in Tab. 1. A spectrum of the form $\kappa^4 exp(-(\kappa/\kappa_0)^2)$ is used for the spectral method. For the vortex method, a tent function $f(x) = 1 - |x|/L$ for all components of velocity in the three directions is used.

The evolution of the turbulent kinetic energy downstream the inlet for all the computations is given on Fig. 1(b). It can be seen that for equivalent length scale of the inflow boundary conditions Fig. 1(a), the spectral methods and the SEM have the same rate of decay. The more the length scale of the inflow data is reduced, the faster the energy is dissipated. The random method does not produce any two-point correlation as can be seen on Fig. 1(a) thus all the energy of the inflow is quickly damped after the inlet. The SEM and spectral method appear to be identical as regards as the evolution of the turbulent kinetic energy. However the energy spectrum corresponding to the SEM does not match exactly that of the spectral method, because the tent function generates more energy at higher wave numbers than the $\kappa^4 exp(-(\kappa/\kappa_0)^2)$ spectrum.

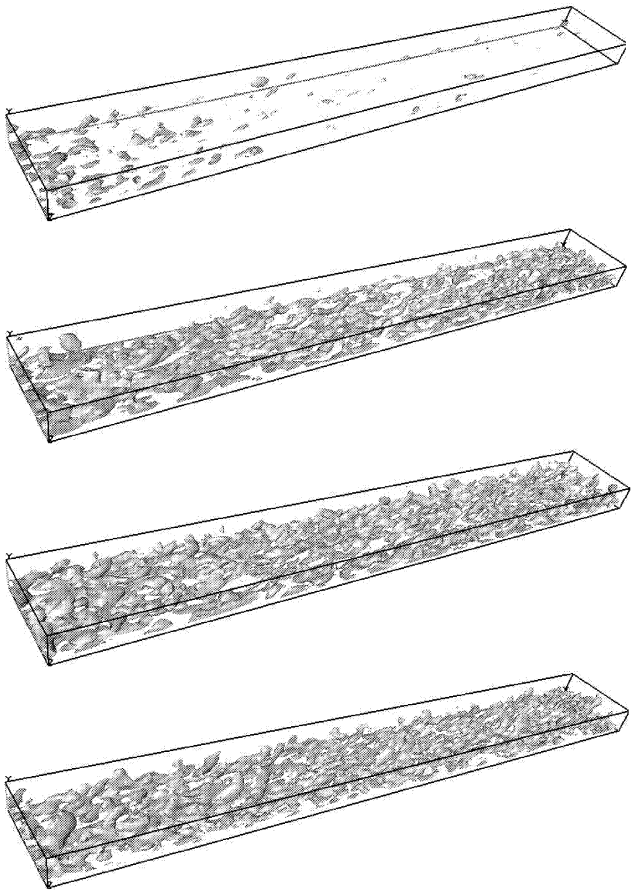

Figure 2: Isoprofiles $Q = 3$ for different methods, from top to bottom computation RAND, SEML02, SPECL02 and PREC

PLANE CHANNEL FLOW

The quality of a synthetic turbulent inlet methodology is measured by its capacity to maintain and/or produce self-sustaining turbulence after the shortest possible development period. The theoretical distance of development after which a laminar flow entering a channel is considered as turbulent is more than 110δ where δ is the channel half width. It was reported (Le et al., 1997) that about 10δ were needed to recover correct intensity levels for a DNS of a turbulent boundary layer

Table 1: Computations for the spatially decaying isotropic turbulence case

Computation	Method	Shape	L
C0SPECL08	Spectral	$\kappa^4 exp(-(\kappa/\kappa_0)^2)$	0.8
C0SPECL04	Spectral	$\kappa^4 exp(-(\kappa/\kappa_0)^2)$	0.4
C0SEML08	SEM	tent function	0.8
C0SEML04	SEM	tent function	0.4
C0RAND	Random	X	0.0

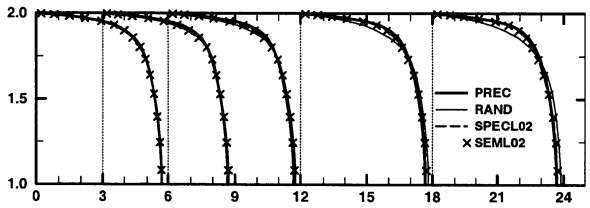

Figure 3: Plane channel flow - Evolution of the mean velocity profiles downstream the inlet for the different methods

with an inflow data generated with a spectral method.

The chosen Reynolds number of $Re^* = 395$ in combination with a fairly coarse mesh makes the case more challenging (real LES rather than quasi DNS). The mesh dimensions are $24\delta \times 2\delta \times 3\delta$ to allow a fully developed flow to establish form the inlet. The number of cells is $160 \times 30 \times 30$ and $\Delta x^+ = 60$, $\Delta y^+_{mean} = 24$, $\Delta y^+_{min} = 1$, $\Delta z^+ = 40$. Periodic boundary conditions are used in the spanwise direction and a no-slip boundary condition is used at the walls. The Smagorinsky constant is set to its recommended value ($C_S = 0.065$) with Van Driest near-wall damping. The various inflow methods are listed in Tab. 2. The so-called precursor simulation uses a periodic simulation carried out on the same mesh; velocity fields from a plane perpendicular to the mean flow were stored and injected at the inlet of our domain. The simulation with the synthetic eddy method SEML01 corresponds to tent functions with a characteristic size of 0.1δ, SEML02 and SEML04 correspond to 0.2δ and 0.4δ. Note that SEML01 correspond roughly to the Prandtl mixing length at the top of the log-layer. However the mesh step in the spanwise direction is $\Delta z = 0.1\delta$ so SEML01 generates the smallest possible structures for the chosen mesh. Case SEMLVR is an attempt to insert a more detailed physical description of channel flow structures: first the length scale is variable and similar to a Prandtl mixing length, also streamwise vortex shape functions are used exclusively in the near wall layer while tent functions generating jettal eddies are used at the centre. A mix of both structures is used in-between. For the spectral method, a spectrum of the form $\kappa^4 exp(-(\kappa/\kappa_0)^2)$ is used over the whole domain (SPECL02). The value of κ_0 is chosen to have the same length and time scale as the simulation (SEML02). All the simulations use the same mean velocity and Reynolds stresses profiles obtained from the periodic calculation.

On Fig. 2, isoprofiles of $Q = \Omega^2 - S^2$ show that SEML02, SPECL02 have realistic wall structures similar to the ones found in PREC whereas in RAND the fluctuations decay continuously. The random method does not manage to produce self-sustaining turbulence whereas the three other methods do. Fig. 3 shows the mean velocity profiles and it can be

Table 2: Computations for the turbulent channel flow case at $Re^* = 395$

Computation	Method	Shape	L_{INT}
SPECL02	Spectral	$\kappa^4 e(-(\kappa/\kappa_0)^2)$	0.2
SEML02	SEM	tent function	0.2
SEML04	SEM	tent function	0.4
SEML01	SEM	tent function	0.1
SEMLVR	SEM	vortices/tent	variable
RAND	Random	X	X
PREC	precursor cal.	X	X

seen that RAND tends towards a more laminar profile. The channel is too short for the mean velocities to be strongly affected by changes in the turbulence shear stresses so we focus on the later. On Fig. 4, PREC shows no streamwise variability as could be expected. Clearly RAND should never be used for channel or boundary layer turbulence. The SEM and the spectral method show very similar results. One cell after the inlet plane, the stresses have lost 30% of their prescribed value. This is certainly due to some adaptations of the synthetic structures to the numerical scheme and Navier-Stokes equations. At $x = 10\delta$ the fluctuations have recovered the levels of the periodic calculation. To remedy the initial loss one could simply overestimate the target stress levels.

Different sizes and shapes of eddies will now be tested to try to reduce the development section. Fig. 5 shows isoprofiles of Q for the smaller (SEML01) and larger (SEML04) inlet structures. As noted previously SEML01 corresponds to structures projected only to spanwise mesh steps. These tend to decay rather than to evolving towards larger scales. In opposition SEML04 starts with too large structures (in comparison to Fig. 2) but in the second half of the channel these are seen to readapt (or possibly generate new structures) with correct lengthscales. Fig. 6 shows that the skin friction coefficient seems to manage to recover its initial value only for SEML04 and SEML02. The structures generated with SEML01 seem too small to generate fully developed turbulence by the end of the domain. The Reynolds stresses are shown on Fig. 7. In the first cell after the inlet plane all four simulations surprisingly lead to the same sudden drop of 30% below the prescribed levels. This would indicate that the issue is not so much a question of adaptation of the imposed structures to the specific numerical scheme (which would be less sensitive in case of larger structures), but perhaps the fact that structures are not divergence free. SEML01 has clearly too small scale structures for the given spanwise resolution. SEMLVR is barely superior for the same reason. Because SEML04 contains large structures easily discretized by the mesh and corresponds too smaller values of dissipation, it was expected that it would develop faster than SEML02 but this is not the case except perhaps at the centre of the channel.

PLANE ASYMETRIC DIFFUSER

The plane asymetric diffuser corresponds to a more industrial case than the two previous ones. Details of the geometry of the case is given in Kaltenback et al. (1999). The Reynolds number based on the friction velocity and the channel half width is $Re^* = 500$. The inlet of the diffuser is a fully de-

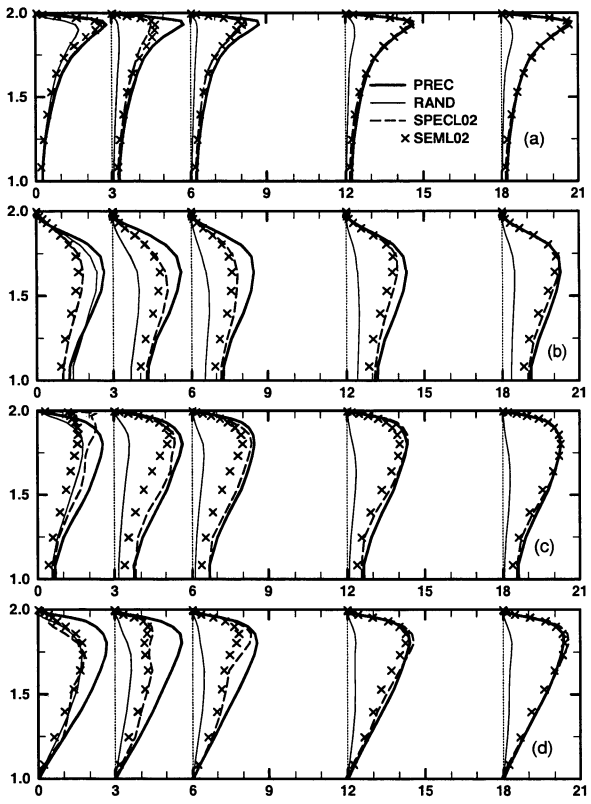

Figure 4: Evolution of the Reynolds stresses profiles downstream the inlet on the top half of the channel for different inflow generation methods, (a) $x + \overline{u^2}/3.5$ (b) $x + \overline{v^2} \times 4$ (c) $x + \overline{w^2} \times 2.2$ (d) $x + \overline{uv} \times 3.5$

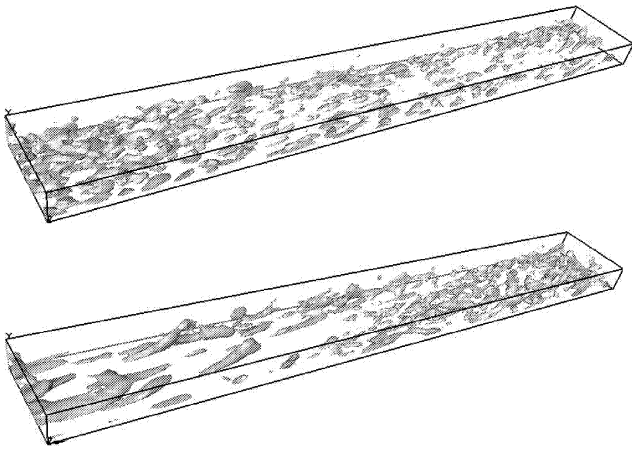

Figure 5: Isoprofiles $Q = 3$ for different size and shape of structure using the SEM, from top to bottom computation SEML01 and SEML04

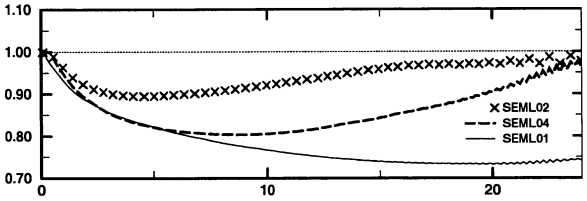

Figure 6: Evolution of the skin friction coefficient $c_f(x)/c_f(0)$ downstream the inlet for different size and shape of vortices - Channel $Re^* = 395$

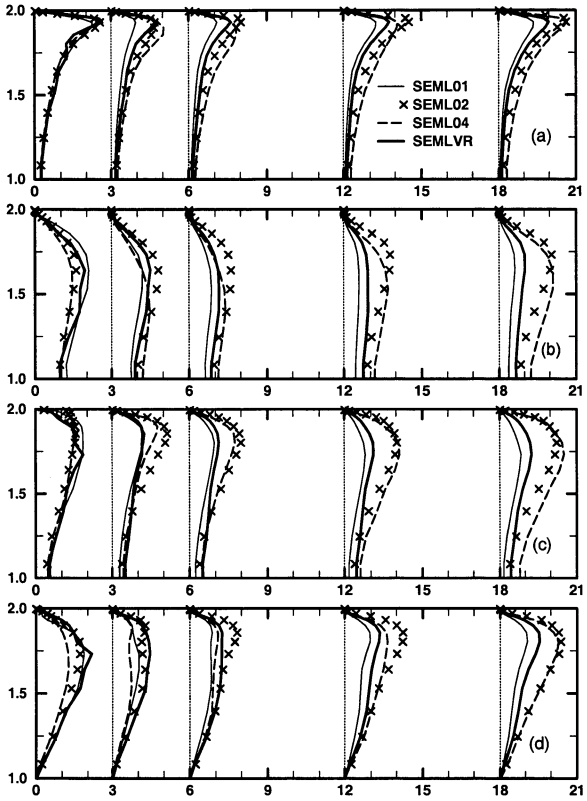

Figure 7: Evolution of the Reynolds stresses profiles downstream the inlet on the top half of the channel $Re^* = 395$ for different size and shape of vortices (a) $x+\overline{u^2}/3.5$ (b) $x+\overline{v^2}\times 4$ (c) $x + \overline{w^2} \times 2.2$ (d) $x + \overline{uv} \times 3.5$

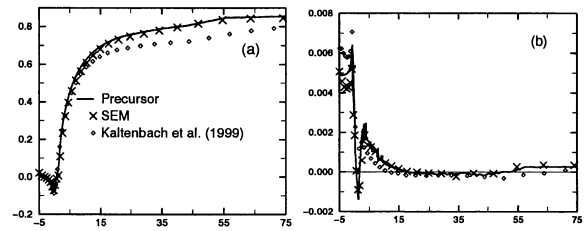

Figure 8: Plane diffuser skin friction and pressure coefficient along deflected wall (a) c_p normalized by U_b (b) c_f normalized by U_b

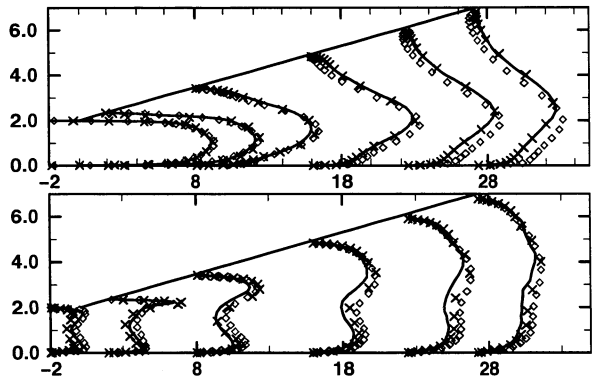

Figure 9: Plane diffuser first part - Mean velocity $x/\delta + 10 \times U/U_b$ (top) and $x/\delta + 50 \times v_{rms}$ (bottom)

veloped turbulent channel flow and is located 5δ before the diffuser throat. The domain used has $272 \times 64 \times 64$ cells and corresponds to the medium LES of Kaltenback et al. (1999). The mesh is refined at both wall in the y direction and around the diffuser throat in the x direction.

Three calculations are carried out, one with a precursor calculation, one with the SEM and one with a basic random method. In the last two cases the mean profiles and energy levels are the one obtained from the precursor calculation. In the case of the vortex method, a tent function is used with the same size of structure as the case SEML02 ($L = 0.2$).

Results are shown on Fig. 8 and 9. The random inlet method fails to reproduce the features of the flow. On the contrary, the precursor calculation and the SEM predict fairly well the separation and reattachment. There is hardly any difference between them. Differences with the Kaltenbach et al. (1999) data can be attributed to the finer mesh, dynamic SGS model and higher order numerical schemes used by the later.

CONCLUSION

A new method for generating turbulent inlet boundary conditions has been developed, presented and compared to existing methods on three test cases. The method is based on the classical view of turbulence as a superposition of eddies. Each eddy is represented by specific shape functions of position and time which describes its spatial and temporal characteristics. The method is able to reproduce specific first and second order one point statistics as well as autocorrelation functions.

Compared to the random method it can produce spatial and temporal correlations which enable to produce fully-developed turbulence in a channel flow a few diameters downstream of the inlet. It gives similar results to the spectral methods for the three test cases simulated but has some advantages over it. It is much faster than the spectral method, enables a better control of the coherent structures within the flow but most of all it is also applicable to completely unstructured grids.

The importance of the size of the structures in the inflow has been shown on the channel case. Further research to find an optimum function describing the coherent structures in the channel flow is being carried out, based proper orthogonal decomposition findings.

AKNOWLEDGEMENTS

The work was partially supported by the EU project DESider, which is a collaboration between Alenia, ANSYS–AEA, Chalmers University, CNRS–Lille, Dassault, DLR, EADS Military Aircraft, EUROCOPTER Germany, EDF, FOI–FFA, IMFT, Imperial College London, NLR, NTS, NUMECA, ONERA, TU Berlin, and UMIST. The project is funded by the European Community represented by the CEC, Research Directorate–General, in the 6th Framework Programme, under Contract No. AST3-CT-2003-502842.

REFERENCES

S. Lee, S. Lele, P. Moin, 1992, "Simulation of spatially evolving compressible turbulence and the application of Taylors hypothesis", *Physics of Fluids*, pp. 1521-1530

T. Lund, X. Wu, D. Squires, 1998, "Generation of turbulent inflow data for spatially-developping boundary layer simulations", *Journal of Computational Physics*, vol. 140, 233-258

M. Klein, A. Sadiki, J. Janicka, 2003, "A digital filter based generation of inflow data for spatially developing direct numerical or large eddy simulations", *Journal of Computational Physics*, vol. 186, 652-665

H. Le, P. Moin, J. Kim, 1997, "Direct numerical simulation of turbulent flow over a backward-facing step", *Journal of Fluid Mechanics*, vol. 330, 349-374

N. Jarrin, S. Benhamadouche, Y. Addad, D. Laurence, 2003, "Synthetic turbulent inflow conditions for large eddy simulation", *Proceedings, 4th International Turbulence, Heat and Mass Transfer Conference*, Antalya, Turkey

K. Kondo, S. Murakami, A. Mochida, 1997, "Generation of velocity fluctuations for inflow boundary conditions of LES", *Journal of Winf Engineering and Industrial Aerodynamics*, vol 67&68, 51-64

F. Archambeau, N. Mehitoua, M. Sakiz, 2004, "Code Saturne: A finite volume Code for the computation of Turbulent Incompressible Flows", *International Journal on Finite Volume*

H.-J. Kaltenbach, M. Fatica, R. Mittal, T.S. Lund, P. Moin, 1999, "Study of flow in a planar asymmetric diffuser using large-eddy simulation", *Journal of Fluid Mechanics*, vol. 390, pp. 151-185 Katenbach

P. Batten, U. Goldberg, S. Chakravarthy, "LNS - An approach towards embedded LES", *AIAA Paper No. 2002-0427*, 40th Aerospace Sciences Meeting and Exhibit, Reno

P. Druault, E. Lamballais, J. Delville, J.-P. Bonnet, 2001, Development of experiment/simulation interfaces for hybrid turbulent results for analysis via the use of DNS, *TSFP2, 2nd International Symposium on Turbulence and Shear Flow Phenomena*, vol. II, Stockholm, 2001, pp. 5-14